0090-9556/09/3708-1785–1791$20.00
DRUG METABOLISM AND DISPOSITION
Vol. 37, No. 8
27201/3490509
DMD 37:1785–1791, 2009
Printed in U.S.A.

Characterization of Sulfoxygenation and Structural Implications of Human Flavin-Containing Monooxygenase Isoform 2 (FMO2.1) Variants S195L and N413K[S]

Sharon K. Krueger, Marilyn C. Henderson, Lisbeth K. Siddens, Jonathan E. VanDyke, Abby D. Benninghoff, P. Andrew Karplus, Bjarte Furnes, Daniel Schlenk, and David E. Williams

Linus Pauling Institute and Department of Environmental and Molecular Toxicology (S.K.K., M.C.H., L.K.S., J.E.V., A.D.B., D.E.W.) and Department of Biochemistry and Biophysics (P.A.K.), Oregon State University, Corvallis, Oregon; and Environmental Toxicology Graduate Program, University of California, Riverside, California (B.F., D.S.)

Received February 18, 2009; accepted April 30, 2009

ABSTRACT:

Catalytically active human flavin-containing monooxygenase isoform 2 (FMO2.1) is encoded by an allele detected only in individuals of African or Hispanic origin. Genotyping and haplotyping studies indicate that S195L and N413K occasionally occur secondary to the functional *FMO2*1* allele encoding reference protein Gln472. Sulfoxygenation under a range of conditions reveals the role these alterations may play in individuals expressing active FMO2 and provides insight into FMO structure. Expressed S195L lost rather than gained activity as pH was increased or when cholate was present. The activity of S195L was mostly eliminated after heating at 45°C for 5 min in the absence of NADPH, but activity was preserved if NADPH was present. By contrast, Gln472 was less sensitive to heat, a response not affected by NADPH. A major consequence of the S195L mutation was a mean 12-fold increase in K_m for NADPH compared with Gln472. Modeling an S213L substitution, the equivalent site, in the structural model of FMO from the *Methylophaga* bacterium leads to disruption of interactions with $NADP^+$. N413K had the same pattern of activity as Gln472 in response to pH, cholate, and magnesium, but product formation was always elevated by comparison. N413K also lost more activity when heated than Gln472; however, NADPH attenuated this loss. The major effects of N413K were increases in velocity and k_{cat} compared with Gln472. Although these allelic variants are expected to occur infrequently as mutations to the *FMO2*1* allele, they contribute to our overall understanding of mammalian FMO structure and function.

Mammalian flavin-containing monooxygenases (FMOs, EC 1.14.13.8) oxygenate many xenobiotics including pharmaceuticals and pesticides that are ingested, inhaled, or otherwise absorbed (Krueger and Williams, 2005). Bound FAD is reduced by equivalents from NADPH and subsequently reacts with molecular oxygen-generating C4a-hydroperoxyflavin intermediate; bound $NADP^+$ stabilizes the intermediate. In the absence of substrate, oxidized flavin and reduced NADPH are slowly regenerated with concomitant release of hydrogen peroxide. However, when substrate possessing a soft nucleophile (primarily N and S but also Se and P) is present, it is quickly oxygenated by the activated intermediate. Oxygenation generally yields less toxic and more readily excreted metabolites; however, bioactivation can also result.

FMOs are a family of related enzymes, each comprising a single isoform. In humans there are five potentially functional FMOs (1–5) and six pseudogenes (Hines et al., 2002; Hernandez et al., 2004). The amino acid sequence identity of encoded isoforms is 51 to 57%. FMO1, FMO2, and FMO3 are the most extensively studied as they are the primary isoforms catalyzing xenobiotic metabolism.

FMO2 is the major FMO in lung of most mammals. However, a g.23238C>T nonsense mutation (*FMO2*2A*) was discovered in humans (Dolphin et al., 1998). The resulting sequence encodes a nonfunctional protein with the premature Q472X stop codon and loss of 64 residues. Because the mutation was absent in chimpanzee and gorilla, the authors concluded that the variant arose following divergence of humans and chimpanzees. Initial genotyping studies documented occurrence of the *FMO2*1* allele encoding Gln472 and full-

This work was supported in part by the National Institutes of Health National Heart, Lung, and Blood Institute [PHS Grant HL038650]; the National Institutes of Health National Institute of Environmental Health Sciences [Grant P30-ES00210]; and the Cell Imaging and Analysis Facility Core and the Proteins Core of the Environmental Health Sciences Center, Oregon State University.

Part of this work was previously presented as follows: Krueger SK, Henderson MC, Siddens LK, VanDyke JE, Furnes B, Schlenk D, and Williams DE (2007) Assessment of methyl *p*-tolyl sulfoxidation by human FMO2.1, p.S195L, and p.N413K flavin-containing monooxygenase variants. *2007 Experimental Biology* meeting; 2007 Apr 28–May 2; Washington, DC. Federation of American Societies for Experimental Biology, Bethesda, MD.

Article, publication date, and citation information can be found at http://dmd.aspetjournals.org.

doi:10.1124/dmd.109.027201.

[S] The online version of this article (available at http://dmd.aspetjournals.org) contains supplemental material.

ABBREVIATIONS: FMO, flavin-containing monooxygenase; PHT, phorate; ANTU, α-naphthylthiourea; SNP, single nucleotide polymorphism; PDB, Protein Data Bank; BVMO, Baeyer-Villiger monooxygenase; ETU, ethylenethiourea; HPLC, high-performance liquid chromatography; MTS, methyl-*p*-tolyl sulfide; MTSO, methyl-*p*-tolyl sulfoxide.

TABLE 1

Minor allele frequency of selected FMO2 SNPs by ancestry

	DNA[a]	Encoded Protein	Ancestry of Individuals					
			African[b]	Hispanic[c]	African[d]	Hispanic[d]	European[d]	Asian[d]
dbSNP Number								
rs2020862	C>**T**	S195L	0.51	0.37	0.46	0.55	0.30	0.52
rs2020865	T>**G**	N413K	0.27	0.11	0.24	0.02	0.02	0.00
rs6661174	**C**>T	Q472X	0.11	0.05	0.20	0.06	0.00	0.00
Individuals			50	153–632	26	20	20	24
Alleles			100	306–1264	52	40	40	48

[a] The ancestral allele is shown first and is followed by the alternative nucleotide. The nucleotide present in the minor allele is underlined and bolded. Note that for Q472X the minor "C" allele is the ancestral allele.
[b] Furnes et al., 2003.
[c] Frequency for occurrence of the allele encoding Gln472 (*FMO2*1*) was made from 632 Hispanic individuals (primarily of Mexican and Puerto Rican ancestry) (Krueger et al., 2004). Estimates for the remaining two alleles (Krueger et al., 2005) were from a subset of the first population, 29 individuals with at least one *FMO2*1* allele and 124 individuals homozygous for *FMO2*2*.
[d] Frequency data from the National Institute of Environmental Health Sciences SNPs database (http://egp.gs.washington.edu).

length active protein exclusively in individuals of either African or Hispanic/Latino descent (Dolphin et al., 1998; Whetstine et al., 2000). The percentage of Hispanic/Latino individuals carrying the *FMO2*1* allele was 2% among Hispanics of Mexican origin and 7% of Hispanics of Puerto Rican origin (Krueger et al., 2004). In the first large African-American cohort examined, 26% of the individuals possessed *FMO2*1* (Whetstine et al., 2000). A recent study stratified nearly 2000 African study subjects by country and documented large variation in *FMO2*1* occurrence with 26 to 50% of sub-Saharan individuals having at least one *FMO2*1* allele (Phillips and Shephard, 2008; Veeramah et al., 2008). Additional missense and nonsense mutations occur, sometimes with high frequency (Whetstine et al., 2000; Furnes et al., 2003; Krueger et al., 2005). However, they are generally predicted to occur secondary to the Q472X truncation (Whetstine et al., 2000; Krueger et al., 2005).

Individuals possessing the *FMO2*1* allele are predicted to exhibit FMO2-dependent xenobiotic metabolism. Overexpressed FMO2.1 efficiently catalyzes oxygenation of a number of xenobiotics, including small thioureas (Henderson et al., 2004b), the thioether insecticides disulfoton and phorate (PHT) (Henderson et al., 2004a), and the antituberculosis prodrug ethionamide (Henderson et al., 2008). Phenylthiourea and α-naphthylthiourea (ANTU) form an intermediate sulfenic acid metabolite capable of glutathione oxidation and FMO-dependent redox cycling, resulting in glutathione depletion in vitro (Henderson et al., 2004b). The primary aim of the current study was to further characterize proteins containing the S195L and N413K missense single nucleotide polymorphisms (SNPs). Both variants are common in individuals of African and Hispanic descent (Furnes et al., 2003; Krueger et al., 2005), whereas only S195L is commonly identified in European and Asian individuals as assessed in the National Institute of Environmental Health Sciences environmental genome project (http://egp.gs.washington.edu) (Table 1). Although haplotype analysis indicates that these mutations are usually secondary to Q472X (Krueger et al., 2005), one individual from a previous study population (Furnes et al., 2003) was homozygous for Gln472 and had the N413K mutation. Because N413K is usually secondary to the S195L variant, we expect that some individuals will also have the S195L mutation on the same chromosome as the Gln472-encoding allele. Both variants retain some activity in vitro (Krueger et al., 2005). In light of the new information on the high occurrence rate of the Gln472 allele in sub-Saharan African populations, understanding the properties of these variants should help us predict the potential impact of these alleles on individual response to xenobiotics and therapeutics. Our secondary aim was to acquire information that would contribute to our understanding of FMO structure and function with the additional insight made possible from the recent crystal structures of FMOs from yeast *Schizosaccharomyces pombe* [Protein Data Bank (PDB) ID codes 1VQW, 2GV8, and 2GVC] (Eswaramoorthy et al., 2006), bacterial *Methylophaga* sp. strain SK1 (PDB ID codes 2VQ7 and 2VQB) (Alfieri et al., 2008), and the related bacterial Baeyer-Villiger monooxygenase (BVMO) and phenylacetone monooxygenase from *Thermobifida fusca* (PDB ID code 1W4X) (Malito et al., 2004).

Materials and Methods

Chemicals. ANTU and ethylenethiourea (ETU) were from Lancaster (Pelham, NH). PHT was purchased from Chem Service, Inc. (West Chester, PA). The remaining chemicals for enzyme assays were purchased from Sigma-Aldrich (St. Louis, MO).

Cloning and Expression of FMO2 Variants. The polymerase chain reaction primers and conditions used to place FMO2 reference cDNA into pENTR (Invitrogen, Carlsbad, CA) and for subsequent creation of S195L and N413K by QuikChange mutagenesis (Stratagene, La Jolla, CA) are documented elsewhere (Krueger et al., 2005). Proteins were produced in Sf9 insect cells as reported there. Microsomes were prepared by differential centrifugation (Krueger et al., 2002) from insect cells harvested 96 h postinfection and were resuspended in storage buffer (10 mM potassium phosphate, pH 7.4, 20% glycerol, 1 mM EDTA, and 100 mM phenylmethylsulfonyl fluoride). Microsomal protein concentrations were determined using Coomassie Plus assay (Pierce, Rockford, IL). The FAD content was measured by high-performance liquid chromatography (HPLC) (Henderson et al., 2004a) to estimate FMO holoenzyme levels for use in subsequent determinations of activity.

Evaluation of Enzyme Activity. Oxidation of methyl *p*-tolyl sulfide (MTS) was analyzed by a published method (Rettie et al., 1990) with some modifications (Siddens et al., 2008). In brief, standard microsomal incubations contained 100 μg of expressed protein (75–200 pmol of FMO) in a total reaction volume of 250 μl (0.1 M tricine, pH 9.0, 1 mM EDTA, and 1 mM NADPH). After 3-min preincubation on ice, reactions were initiated by adding MTS to 200 μM and transferred to a Dubnoff shaking incubator (Precision Scientific, Winchester, VA) at 37°C. Reactions were stopped after 5 min by placing the tubes on ice and adding 75 μl of acetonitrile to precipitate proteins. After centrifugation at 10,000*g* for 30 min at 4°C, supernatants were analyzed by HPLC with a Waters (Milford, MA) 2695 system equipped with a photodiode array detector. Methyl *p*-tolyl sulfoxide (MTSO) was separated from MTS on a Waters Novapak C_{18} (150 × 3.9 mm) column at 40°C with a flow rate of 0.8 ml/min and detection at 237 nm. Mobile phase was 30% acetonitrile for 4 min to 80% acetonitrile in 2 min and returned to 30% acetonitrile at 8 min in 2 min. Racemic MTSO and MTS eluted at 2.7 and 8.7 min, respectively. MTSO formation was calculated by linear regression from standard curves ($r^2 = 0.997$) of racemic MTSO (0.5–5 nmol) with a detection limit of 50 pmol.

The effects of previous mild heat treatment or the presence of additives to the standard reaction mixture on activity were determined by measuring changes in MTSO formation as already described above. Samples were prepared for assessment of heat stability by dilution with storage buffer to 3 mg of protein/ml and were heated (5 min at 45°C) in the absence or presence of NADPH (1 mM); samples were chilled on ice, and reaction mixtures were

prepared for assessment of activity. The effects of sodium cholate (0.5%) and magnesium chloride (3 mM) on FMO2 variant performance were assessed by their respective addition to the reaction mixture just before the 3-min preincubation on ice. Three batches of protein and at least two assays per batch for each variant were performed for each condition. A pH of 9.0 was selected for assays because FMO2s typically exhibit enhanced activity at this pH compared with pH 7.5.

The activity of protein variants was compared at three pH levels (8.5, 9.0, and 9.5) with MTS, ANTU, and PHT to determine whether all the proteins showed the same response pattern toward different substrates. MTS assays were performed as described above with 200 μM MTS and 5-min incubation. Reactions for oxygenation of ANTU and PHT were performed as with MTS oxygenation, but the reaction mixture volume was reduced to 100 μl. Reactions were stopped by addition of 50 μl of methanol following 10-min incubation. Supernatants were analyzed by HPLC as previously described for ANTU (Henderson et al., 2004b) and PHT (Henderson et al., 2004a). In those studies, liquid chromatography/mass spectrometry was used to show that the sole metabolites formed from ANTU and PHT are the sulfenic acid and the *S*-oxide, respectively. However, as authentic standards were not available for these metabolites, metabolite formation is reported here as peak area per picomole of FMO. The substrate concentrations for ANTU and PHT were 200 and 500 μM, respectively. Three batches of protein and at least two assays per batch for each variant were performed for each condition.

Kinetic constants were determined for MTS oxygenation and NADPH oxidation. Studies were performed at pH 9.0 to be consistent with earlier estimates made for ETU metabolism (Krueger et al., 2005). For determination of kinetics of MTS oxygenation, 50 to 70 μg (50–150 pmol of FMO) of expressed microsomal protein was incubated in a 1-ml reaction (0.1 M tricine, 1 mM EDTA, and 1 mM NADPH). After 3-min preincubation on ice, reactions were initiated by adding MTS (0.6–200 μM for FMO2.1 and N413K; 10–200 μM for S195L). Samples were shaken 4.5 min at 37°C and stopped by addition of 2 ml of ethyl acetate. Samples were vortexed 1 min; the ethyl acetate fraction was transferred to a new tube; and the extraction was repeated. Combined ethyl acetate fractions were brought to dryness in a SpeedVac (Thermo Fisher Scientific, Waltham, MA). The reaction products were resuspended in 100 μl of mobile phase, and 50 μl was analyzed by HPLC as described above. NADPH oxidation was determined in 1 ml of reaction buffer (0.1 M tricine, pH 9.0, 1 mM EDTA) that contained 100 μg of protein (75–200 pmol of FMO), 200 μM MTS, NADPH (5–1000 μM for all the proteins), and an NADPH-regenerating system (2 mM glucose 6-phosphate and 0.25 U of glucose-6-phosphate dehydrogenase). The reaction time was 2 min, followed by termination with 75 μl of acetonitrile on ice. MTSO generated was analyzed in 100-μl aliquots with the HPLC procedure described above. Two to three batches of protein were used for each protein, with six concentrations of NADPH. Kinetic constants were estimated using nonlinear regression curve fitting with the Michaelis-Menten module of GraphPad Software Inc. (San Diego, CA) Prism 5.0.

Statistical Analysis. Enzyme activity of the variant proteins was compared with FMO2.1. For kinetic studies this comparison was done using simple unpaired *t* tests given that the replication level was low ($n = 2$ or 3 batches of each protein). Because of the small sample size, assumptions of the *t* test (e.g., normal data, equality of variance) were not assessed. Two-way analysis of variance was used to analyze the effects of protein variant and pH with ANTU, PHT, or MTS as substrate, as well as the effects of additives and heat pretreatment. Appropriate post hoc pair-wise comparisons were made using a *t* test with a Bonferroni adjustment. SigmaStat version 2.03 (Systat Software, Inc., San Jose, CA) was used for these calculations.

FMO Sequence Alignments and Structural Evaluation. FMO sequences were searched for and identified in either nucleotide or protein databases at the National Center for Biotechnology Information (http://www.ncbi.nlm.nih.gov/sites/gquery) or Ensembl genome databases (http://www.ensembl.org/index.html) to prepare alignments to assess conservation of residues under study. Only unambiguous sequences capable of encoding full-length proteins were included. The only exceptions to this inclusion were *FMO2* genes that, although complete, appeared to encode prematurely truncated proteins. All the deposited mammalian sequences (isoforms 1–5) and a noninclusive sampling of more distantly related vertebrate FMOs were included. Variant protein sequences were not included in the alignment, except for known FMO2 truncations. A limited number of nonvertebrate eukaryotes were selected to represent a broad spectrum of FMO evolution, but choices were restricted to FMOs known to produce transcribed message and/or protein. Bacterial FMOs were limited to species that have been characterized in vitro. The sampling strategy was done to achieve maximal depth of coverage for mammalian isoforms, as well as a broad shallow sampling of distantly related FMOs for examination of evolutionary conservation at positions homologous to the variants under study. All the sequences evaluated are listed as a supplement to this article (Supplemental Table S1). Sequences were prepared in FASTA format and submitted for on-line ClustalW2 analysis from the EBI web server (http://www.ebi.ac.uk/Tools/clustalw2/) using default settings (Larkin et al., 2007).

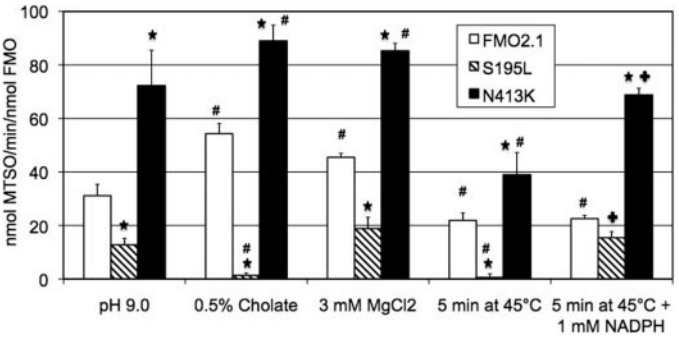

FIG. 1. Metabolite formation resulting from oxidation of MTS at pH 9.0 by FMO2 variants shows treatment by variant dependence. Error bars indicate S.D. ∗, comparisons for the test that variants are significantly different from FMO2.1 within a given treatment. #, significant differences for the test of treatment within a variant versus activity at pH 9.0. +, significant differences for the test of presence of NADPH during heat treatment within a variant versus NADPH absence.

The structural location and consequence of S195L and N413K variants were evaluated by swapping human FMO2 residues with the corresponding residues of *Methylophaga* sp. FMO (PDB code 2VQ7). PyMOL visualization software (The PyMOL Graphics System; DeLano Scientific, Palo Alto, CA) was used for analysis and figure rendering.

Results

Modulators of FMO Activity. Expressed FMO2.1, S195L, and N413K were evaluated in vitro under a number of conditions commonly used to discriminate FMO isoforms; FMO2s are generally heat-stable and show enhanced enzymatic activity with anionic detergents (Williams et al., 1985). Results are shown in Fig. 1. FMO2.1, reference protein encoding Gln472, responded with a highly significant ($p < 0.01$) mean 74 and 46% increase in activity with the addition of cholate and $MgCl_2$, respectively. After 5 min of heat, FMO2.1 retained 70% activity ($p < 0.01$) in the absence of NADPH and 73% activity ($p < 0.05$) in the presence of NADPH, relative to unheated protein. As addition of NADPH did not enhance activity of FMO2.1, thermal stability was NADPH-independent.

The pattern of response by N413K to the same treatments was generally similar to that of FMO2.1, albeit of differing magnitudes. Compared with N413K activity at pH 9.0, cholate and $MgCl_2$ pretreatment resulted in significant ($p < 0.01$) increases: 23 and 18%, respectively. Inactivation by heat treatment without NADPH was highly significant ($p < 0.01$), leading to a 46% loss in activity. However, in contrast to FMO2.1, N413K activity was preserved by NADPH and did not show a decrease in activity following heat pretreatment. The amount of MTSO formed by N413K was much higher ($p < 0.01$) than the amount formed by FMO2.1 for every treatment.

S195L showed a unique pattern of response to the treatments. $MgCl_2$ did not increase activity ($p = 0.35$), and most activity, 89%, was lost by cholate treatment ($p < 0.01$), responses in stark contrast

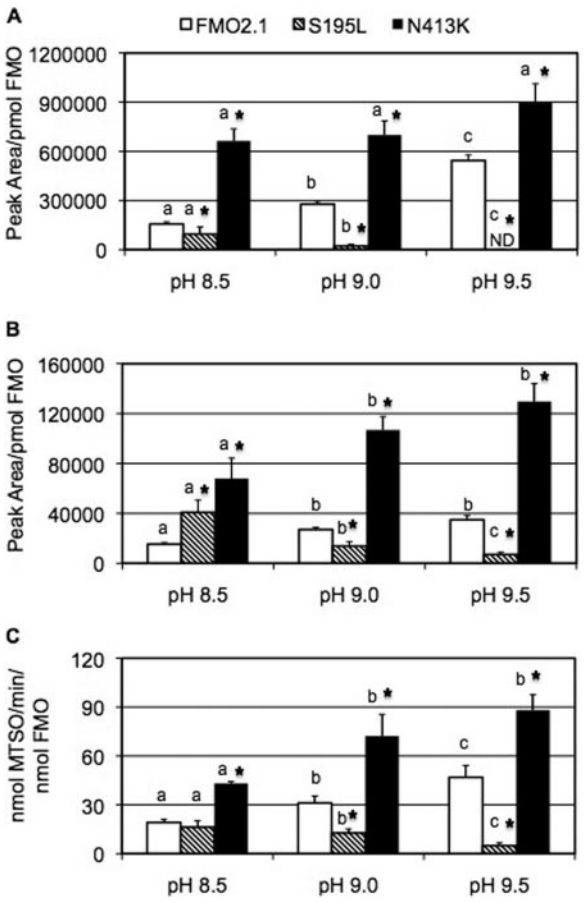

FIG. 2. Metabolite formation resulting from oxidation of ANTU (A), PHT (B), and MTS (C) by FMO2 variants shows pH by variant dependence. Error bars indicate S.D. Statistically significant differences for the test of pH within a variant are distinguished by different letters (a, b, c), and * indicates significance for the test that variant proteins are different from FMO2.1, within a single pH. ND, none detected.

to the pattern observed with both FMO2.1 and N413K. Heat treatment of S195L in the absence of NADPH resulted in a 95% loss of activity ($p < 0.01$). However, coincubation with NADPH during heat exposure rescued S195L activity. The only conditions where S195L activity was not significantly less than that of FMO2.1 were when samples were heated in the presence of NADPH.

Activity of FMO2 isoforms typically increases as pH is elevated above physiological levels, achieving maximal activity at approximately pH 9.5 to 10, a pattern first shown for rabbit FMO2 (Williams et al., 1985). Human FMO2.1 illustrates this pattern of metabolism when methimazole is the substrate (Krueger et al., 2002). As shown in Fig. 2, activity of FMO2.1 increased for each of three substrates as pH was elevated, although activity reached a plateau at pH 9.0 when PHT was the substrate. We evaluated S195L and N413K with the same conditions to determine whether they exhibited the same pattern of activity in response to changing pH (Fig. 2). N413K activity was higher ($p < 0.01$) than FMO2.1 activity at every pH with all the substrates. Although a pattern of increased activity with elevated pH was observed with all the substrates, activity always reached a plateau at pH 8.5 (ANTU) or pH 9.0 (PHT and MTS), indicating that the incremental response to pH by the N413K variant was less than that of FMO2.1.

The behavior of S195L was in distinct contrast to FMO2.1 and N413K. S195L showed maximal activity at pH 8.5, the lowest pH tested. Activity achieved by S195L at pH 8.5 was significantly less than that of FMO2.1 only with ANTU and was significantly ($p < 0.01$) higher than FMO2.1 when PHT was the substrate. As pH was increased, S195L activity decreased significantly ($p < 0.01$) with all the substrates, with each incremental pH increase. S195L was significantly ($p < 0.01$) less active than FMO2.1 at pH 9.0, the pH used for initial screening of activity (Krueger et al., 2005).

TABLE 2

Kinetic parameters for FMO2.1, S195L, and N413K (mean ± S.D.)

Kinetic values significantly (*, $p \leq 0.05$) or highly significantly (**, $p \leq 0.01$) different than FMO2.1.

Variant	K_m	k_{cat}	k_{cat}/K_m
	μM	*nmol substrate/min/nmol FMO*	
MTS			
FMO2.1	13.5 ± 5.2	42.3 ± 6.8	3.3 ± 0.8
S195L	5.0 ± 2.2	10.0 ± 0.2*	2.2 ± 0.9
N413K	4.8 ± 0.5	71.1 ± 1.3**	14.9 ± 1.9*
NADPH			
FMO2.1	11.5 ± 14.2	23.6 ± 9.9	6.8 ± 8.1
S195L	132 ± 72.8*	15.2 ± 2.9	0.14 ± 0.07
N413K	6.8 ± 2.3	94.4 ± 9.9**	14.4 ± 3.3

Kinetic Parameters. Kinetic constants were determined for MTS oxygenation (Table 2). The k_{cat} of S195L was almost 3-fold lower ($p < 0.05$) than FMO2.1. Both proteins had high affinity for MTS, and although the K_m of S195L was lower, it did not reach the threshold of significance. Because low reaction velocity limited MTSO formation by S195L, we did not run MTS assays at concentrations less than 10 μM. Although we are confident that the true K_m of S195L is less than 10 μM, our estimate may contain some unaccounted for error; nonetheless, it is not likely to be significantly different from FMO2.1. The K_m for N413K was very similar to that of S195L but was not significantly different from that of FMO2.1. However, the k_{cat} for MTS oxygenation by N413K was significantly higher ($p < 0.01$) with this variant. Overall catalytic efficiency of N413K was significantly higher ($p < 0.05$) than that of FMO2.1.

Kinetic constants for NADPH use with MTS as substrate were also determined (Table 2). The K_m values for NADPH affinity by FMO2.1 and N413K were low (11.5 and 6.8 μM, respectively), indicating both have high affinity; calculated affinities were not significantly different. These affinities were slightly higher than those of pig FMO1 (1.0–6.5 μM), the only other mammalian FMO with NADPH affinity data, using a variety of substrates and a range of pH (7.4–8.5) (Poulsen and Ziegler, 1979; Beaty and Ballou, 1981; Sabourin and Hodgson, 1984). The k_{cat} of N413K was significantly higher than that of FMO2.1. The specificity constant of N413K was not significantly elevated compared with FMO2.1, primarily because of the high deviation we had among FMO2.1 batches ($n = 3$). Nonetheless, it is clear that k_{cat} is the improved feature of this variant, which we reported previously using ETU as the test substrate (Krueger et al., 2005). The k_{cat} of S195L was no different from that of FMO2.1. By contrast, the affinity of S195L for NADPH was significantly compromised as shown by a mean 12-fold elevation of K_m ($p < 0.05$) compared with FMO2.1. The elevated K_m that we measured with S195L is similar to the 9-fold increase observed with the K219A mutant of Baker's yeast (Suh et al., 1999), located near the GxGxxG/A NADPH-binding motif (Supplemental Fig. S1). The specificity constant of S195L did not differ significantly from that of FMO2.1.

We verified that k_{cat} estimates for individual proteins did not differ significantly under the two sets of assay conditions. In addition, we verified that k_{cat} estimates of 41 and 124 min^{-1} previously reported for metabolism of ETU by FMO2.1 and N413K, respectively, are reasonably similar with the estimates reported in Table 2. All of the

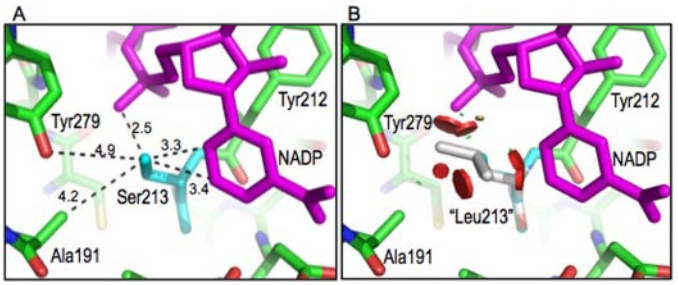

FIG. 3. The consequences of an S195L mutation. A, in the crystal structure of *Methylophaga* sp. FMO (PDB code 2VQ7), Ser213 (the equivalent of Ser195 in human FMO2) is intimately involved in $NADP^+$ binding (short hydrogen bond to atom O2N of the $NADP^+$ pyrophosphate and van der Waals contacts with the nicotinamide Cβ atom of Ala191 (equivalent to Ser173 in human FMO2, which has an even larger side chain). B, replacing Ser213 with Leu in the *Methylophaga* sp. structure leads to major collisions (red disks) with atoms of $NADP^+$ and Ala191, explaining why this mutation is highly disruptive to $NADP^+$ binding. Analysis done and figure created with PyMOL.

k_{cat} estimates (of a given isoform or variant) were consistent with the catalytic mechanism of flavin-containing monooxygenases. This mechanism dictates that all the substrates that gain access to the active site will do so with a similar k_{cat} because FMOs generate activated and relatively stable C4a-hydroperoxy flavin intermediate independent of substrate binding.

Sequence and Structural Evaluation. We assembled and aligned 89 unique FMO sequences (Supplemental Table S1) from GenBank and Ensembl. Sequence coverage included 66 mammalian, two bird, four amphibian, three fish, one insect, five nematode, three plant, two yeast (fungal), and three bacterial FMOs (two that are BVMOs). For the purpose of this article, phenylacetone monooxygenase from *T. fusca* was treated as an FMO because it is a closely related BVMO and crystals have been obtained (Malito et al., 2004). The two FMOs that have yielded crystals—yeast FMO from *S. pombe* (Eswaramoorthy et al., 2006) and bacterial FMO from *Methylophaga* FMO (Choi et al., 2003; Alfieri et al., 2008)—are included. All the sequences used in the alignment are class B flavoprotein monooxygenases (van Berkel et al., 2006).

Conserved strand-turn-helix motifs (GxGxxG for FAD and GxGxxG/A for $NADP^+$) are known to stabilize nucleotide binding. This role was verified by the observed residue interactions from the crystal structure of *S. pombe* FMO (Eswaramoorthy et al., 2006). The Ser encoded by residue 195 in human FMO2 is within the $NADP^+$ motif (GxGx*S*G/A) and is highly conserved among FMOs (76 of 89) (Supplemental Fig. S1). The only exceptions to this use were that most FMO4s (11 of 13) and *Mycobacterium tuberculosis* use Thr instead of Ser, whereas primate FMO1 incorporates Pro. It is interesting to note that Ser conservation also extends to the analogous position of the FAD binding motif (GxGx*S*G), where 87 of 89 proteins incorporate Ser, whereas the remaining two FMOs use Thr and Ala (Supplemental Fig. S1).

Extensive conservation of Ser across evolutionary distance implies conservation of a structural role and indicates that examination of Leu substitution in the structural model derived from crystals of *Methylophaga* sp., *S. pombe*, or *T. fusca* could explain the basis for our observation of reduced affinity for NADPH and high loss of enzyme activity when the Leu-containing variant is heated (in the absence of NADPH). Figure 3A visualizes the interactions of Ser213 in the *Methylophaga* sp. FMO crystal (PDB code 2VQ7) (Alfieri et al., 2008), the equivalent of Ser195 in human FMO2.1. Ser213 interacts with bacterial Ala191, Tyr212, and Tyr279. Replacement of Ser with Leu213 (Fig. 3B) would lead to disruption of interactions with all the indicated residues and $NADP^+$, indicating that the effects of S195L substitution are direct and are not simply the result of a shift in an important neighboring residue. The contact residues are also indicated in Supplemental Fig. S1.

The interacting residues are in critical regions. Tyr212 has been singled out for its involvement, together with $NADP^+$, in blocking solvent access to reduced FAD and the catalytic core (Alfieri et al., 2008). The FMOs of most eukaryotes use Asn instead of Tyr; Tyr212 corresponds to Asn194 of human FMO2.1. Ala191 is in the FMO signature motif FxGxxxH*x*xxF/Y (at the italicized residue) (Fraaije et al., 2002) and corresponds to residue 173 in human FMO2.1. Human FMO2.1 uses Ser at this site as do the majority (83 of 89 FMOs) of the FMOs examined (Supplemental Fig. S1). It is interesting to note that a mutagenesis study performed with cyclohexanone monooxygenase, a BVMO from *Acinetobacter* sp. NCIB 9871, showed that mutagenesis of the conserved His in the signature motif also resulted in a doubling of the K_m for NADPH binding compared with wild-type enzyme (Cheesman et al., 2003). *Methylophaga* Tyr279 corresponds to human FMO2.1 Tyr331. This Tyr is the final residue of the prototypic "FATGY" motif; this motif is highly conserved among all the FMOs aligned except for the BVMOs from *T. fusca* and *M. tuberculosis*. As reviewed elsewhere (Krueger and Williams, 2005), the FATGY motif has also been variously identified as the ATG_{NADPH} motif (E/DxxxxATG) found in flavoproteins with two nucleotide binding domains, and it overlaps two PRINTS motifs known to form a linkage between the $NADP^+$ binding domain and active site of relevant proteins.

With the number of disruptions predicted by the S195L substitution it is not surprising that we observed altered enzyme performance with this FMO2 variant. The Leu195-Ser173 collisions are expected to distort the structure and thermodynamically destabilize the protein, explaining the greater heat lability of this mutant. NADPH binding to the mutant partly salvages the activity because the favorable interactions with NADPH make the complex have slightly higher stability than the empty mutant enzyme. Stabilization of enzyme activity and structure by cofactor or substrate binding is a common theme. Studies of the BVMO, 4-hydroxyacetophenone monooxygenase, showed that when NADPH was included with 4-hydroxyacetophenone monooxygenase during heat treatment, activity, FAD binding, and quaternary structure were maintained. However, FAD was lost, protein became aggregated, and activity was lost when this protein was heated in the absence of NADPH (van den Heuvel et al., 2005). Thus, the C4a-hydroperoxy flavin of S195L may not only be subject to solvent attack but also subsequent loss of FAD and aggregation.

The N413K substitution improves enzyme velocity and subsequently calculated specificity constants for the substrates examined but does not fundamentally change the direction of response to treatments such as pH, detergent, and $MgCl_2$. Alignment of multiple FMO sequences reveals that this region and site vary in an isoform-specific manner (Supplemental Fig. S1). Whereas FMO2s use Asn, FMO1s use Lys and FMO3s and FMO6s generally use Met at the position equivalent to N413K of human FMO2. The analogous *Methylophaga* FMO site is Arg361 and is on the surface of a monomer far from the active site. Crystallized *Methylophaga* FMO is a tetramer, and Arg361 is at the interface between two subunits where it interacts directly with one of the other chains near Lys32 (data not shown). In the absence of a crystal structure from a mammalian FMO, it is not clear why N413K enhances enzyme velocity.

It has been suggested that human FMO2 is en route to becoming a pseudogene (Phillips and Shephard, 2008), but this phenomenon may not be limited to humans. In addition to work describing the occurrence and functional outcomes of the common human FMO2 Q472X nonsense mutation (Dolphin et al., 1998; Whetstine et al., 2000; Krueger et al., 2004), there is also work describing a common variant

of the Norway rat (deletion of two nucleotides results in a frame shift) (Hugonnard et al., 2004). In the course of assembling additional mammalian FMO2 sequences for alignment, we found an uncharacterized variant in the sole sequence located for *Bos taurus* (Supplemental Fig. S1). Cow FMO2 truncation results from an extended C-terminal deletion. It is not known whether this deletion is fixed or segregating in cows or other closely related species, but this deletion seems to be the third case of a species losing or being in the process of losing functional FMO2. The cow and Norway rat each have a unique truncation position encoding proteins even shorter than human FMO2. Given that human Q472X does not bind FAD (Krueger et al., 2002), neither cow nor Norway rat FMO2 is expected to generate FAD-bound enzyme. One of the alleles responsible for trimethylaminuria is the human FMO3 variant encoding R492W, an inactive protein that does not bind FAD (Yeung et al., 2007). Homology modeling with *S. pombe* FMO places Arg492 in close proximity to its FAD catalytic center, Asn61 (Yeung et al., 2007). All mammals use Arg at this position, and most eukaryotes retain a positively charged residue (Supplemental Fig. S1). It is clear that loss of Arg494, the analogous residue from human FMO2, would be sufficient to prevent FAD binding by Q472X, although other crucial elements may also reside in this region.

Discussion

The studies in this report show that the FMO2 S195L variant expressed on a Gln472 background is less detrimental than we had previously thought (Krueger et al., 2005), primarily owing to improved enzyme activity when pH is reduced. Our study provides evidence that NADPH, although not capable of forming ideal interactions, nonetheless gives S195L some added stability and preserves some activity. We do not expect that S195L would have the enzymatic stability or activity of wild-type FMO2 under physiological conditions. Evidence of S195L impairment is not limited to thermal sensitivity documented here. We have also observed elevated hydrogen peroxide leakage with the S195L variant compared with FMO2.1 and N413K in reaction mixtures containing NADPH at physiological pH (L. K. Siddens, S. K. Krueger, and D. E. Williams, unpublished studies). Elevated leakage fits the expected shift toward NADPH oxidase activity as a decay product of solvent-exposed C4a-hydroperoxyflavin intermediate when NADPH is weakly bound. NADPH-dependent retention of S195L activity to heat and H_2O_2 leakage data both imply that the reduced flavin is less protected from oxygen in this variant. This leakage is consistent both with destabilization of the structure in the NADPH binding region as indicated by substitution into the crystal structure of *Methylophaga* and the reduced binding affinity calculated for NADPH from kinetic studies.

Inferences about the role of N413K are necessarily limited because this polymorphism lies in a region that is rich in isoform-specific differences. Presumably N413K is optimized for regeneration of FAD via release of water from FAD-OH and/or release of $NADP^+$, because these are the two slowest steps of the catalytic cycle. Given that FMO1 isoforms use Lys rather than Asn, we would predict a K413N mutation would generate an FMO1 variant with less activity and reduced k_{cat}. Definitive assignment of function will require crystal structure information from a higher organism than is presently available.

Owing to the wide distribution of the *FMO2*2* allele, S195L and N413K are expected to yield functional protein only if they are present in combination with the minor *FMO2*1* allele in individuals of either African or Hispanic descent. Recent work (Phillips and Shephard, 2008; Veeramah et al., 2008) has shown that in some sub-Saharan African populations *FMO2*1* can be present in 26 to 50% of the population, levels previous studies had failed to appreciate owing to lack of information on organ donor origin. Consequently, there are approximately 220 million individuals in sub-Saharan Africa that may express functional protein (Veeramah et al., 2008). Individuals with SNPs encoding either active N413K (known to exist) or S195L (probably exists) secondary to Gln472 are expected with the highest frequency in these populations.

Codistribution of tuberculosis incidence and *FMO2*1* occurrence could have profound implications for the treatment of this prevalent disease. A number of tuberculosis treatments, such as ethionamide and thiacetazone, are prodrug substrates of the *M. tuberculosis* FMO, EtaA, and are also excellent substrates of human FMO2.1 (Henderson et al., 2008; Francois et al., 2009). Metabolism of ethionamide by FMO1, FMO2.1, and FMO3 in vitro alters the GSSG/GSH ratio (Henderson et al., 2008), suggesting that redox cycling and GSH depletion may result in vivo in an *FMO2*1*-dependent manner in lung. Further study is warranted because co-occurrence of FMO2.1 and mycobacterial EtaA could affect both the rate of adverse clinical reactions and efficacy of mycobacterial eradication.

Individuals receiving pharmaceutical treatment for genetic disorders caused by nonsense mutations are a new group of individuals that may be expressing functional FMO2 protein. PTC Therapeutics (South Plainfield, NJ) has developed a stop codon read-through drug, PTC124 (Welch et al., 2007). In theory, PTC124 will produce full-length protein from all the mRNAs possessing a premature termination codon caused by a nonsense mutation. Thus, treated individuals with the allele for the major FMO2 SNP Q472X could express active FMO2 protein and secondary S195L and N413K SNP-encoding variants. To date, PTC124 has been administered to normal individuals in phase 1 tests and to patients with cystic fibrosis and Duchenne or Becker muscular dystrophy in phase 2 tests. Although the number of individuals receiving this drug now and in the future will probably remain small, the number of diseases tested with this drug regimen is likely to grow. Patients taking PTC124 may develop altered patterns of drug and xenobiotic metabolism as a result of read-through of the Q472X-encoding allele, *FMO2*2*, and any secondary variants yielding FMO2 with substantial activity. The existence of this subpopulation with newly "acquired" functional FMO2 adds to the necessity that we understand the properties of what are usually secondary mutations, given that they will be uncovered in patients taking this class of drugs.

Strides have been made in understanding the structure and function of mammalian FMO. Channel length and width of substrate binding sites were established with substituted thioureas and phenothiazines, and isoform-dependent differences were identified using substrate probes (Nagata et al., 1990; Guo et al., 1992; Shehin-Johnson et al., 1995; Kim and Ziegler, 2000). Study of trimethylaminuria-causing gene products marked the earliest efforts to understand naturally occurring human FMO mutations; such studies have confirmed more than 30 rare causative mutations (Phillips and Shephard, 2008) (the 17 documented missense mutations are indicated in Supplemental Table S1), in addition to more common SNPs that may mildly reduce enzyme activity. In some studies, the basis of activity reduction was identified for the expressed protein variants and was attributed to no or reduced FAD cofactor binding, altered K_m or k_{cat}, or both. More recently, structural data from crystallized yeast and bacterial FMOs have provided further insight regarding the structural basis of functional FMO3 variants (Eswaramoorthy et al., 2006; Koukouritaki et al., 2007; Yeung et al., 2007; Alfieri et al., 2008). We expect that these studies will continue to add structure-function knowledge; however, the biggest informational and predictive gains still await successful crystallization of a mammalian FMO.

References

Alfieri A, Malito E, Orru R, Fraaije MW, and Mattevi A (2008) Revealing the moonlighting role of NADP in the structure of a flavin-containing monooxygenase. *Proc Natl Acad Sci U S A* **105:**6572–6577.

Beaty NB and Ballou DP (1981) The reductive half-reaction of liver microsomal FAD-containing monooxygenase. *J Biol Chem* **256:**4611–4618.

Cheesman MJ, Byron Kneller M, and Rettie AE (2003) Critical role of histidine residues in cyclohexanone monooxygenase expression, cofactor binding and catalysis. *Chem Biol Interact* **146:**157–164.

Choi HS, Kim JK, Cho EH, Kim YC, Kim JI, and Kim SW (2003) A novel flavin-containing monooxygenase from *Methylophaga* sp strain SK1 and its indigo synthesis in *Escherichia coli*. *Biochem Biophys Res Commun* **306:**930–936.

Dolphin CT, Beckett DJ, Janmohamed A, Cullingford TE, Smith RL, Shephard EA, and Phillips IR (1998) The flavin-containing monooxygenase 2 gene (FMO2) of humans, but not of other primates, encodes a truncated, nonfunctional protein. *J Biol Chem* **273:**30599–30607.

Eswaramoorthy S, Bonanno JB, Burley SK, and Swaminathan S (2006) Mechanism of action of a flavin-containing monooxygenase. *Proc Natl Acad Sci U S A* **103:**9832–9837.

Fraaije MW, Kamerbeek NM, van Berkel WJ, and Janssen DB (2002) Identification of a Baeyer-Villiger monooxygenase sequence motif. *FEBS Lett* **518:**43–47.

Francois AA, Nishida CR, de Montellano PR, Phillips IR, and Shephard EA (2009) Human flavin-containing monooxygenase 2.1 catalyzes oxygenation of the antitubercular drugs thiacetazone and ethionamide. *Drug Metab Dispos* **37:**178–186.

Furnes B, Feng J, Sommer SS, and Schlenk D (2003) Identification of novel variants of the flavin-containing monooxygenase gene family in African Americans. *Drug Metab Dispos* **31:**187–193.

Guo WX, Poulsen LL, and Ziegler DM (1992) Use of thiocarbamides as selective substrate probes for isoforms of flavin-containing monooxygenases. *Biochem Pharmacol* **44:**2029–2037.

Henderson MC, Krueger SK, Siddens LK, Stevens JF, and Williams DE (2004a) S-oxygenation of the thioether organophosphate insecticides phorate and disulfoton by human lung flavin-containing monooxygenase 2. *Biochem Pharmacol* **68:**959–967.

Henderson MC, Krueger SK, Stevens JF, and Williams DE (2004b) Human flavin-containing monooxygenase form 2 S-oxygenation: sulfenic acid formation from thioureas and oxidation of glutathione. *Chem Res Toxicol* **17:**633–640.

Henderson MC, Siddens LK, Morré JT, Krueger SK, and Williams DE (2008) Metabolism of the anti-tuberculosis drug ethionamide by mouse and human FMO1, FMO2 and FMO3 and mouse and human lung microsomes. *Toxicol Appl Pharmacol* **233:**420–427.

Hernandez D, Janmohamed A, Chandan P, Phillips IR, and Shephard EA (2004) Organization and evolution of the flavin-containing monooxygenase genes of human and mouse: identification of novel gene and pseudogene clusters. *Pharmacogenetics* **14:**117–130.

Hines RN, Hopp KA, Franco J, Saeian K, and Begun FP (2002) Alternative processing of the human FMO6 gene renders transcripts incapable of encoding a functional flavin-containing monooxygenase. *Mol Pharmacol* **62:**320–325.

Hugonnard M, Benoit E, Longin-Sauvageon C, and Lattard V (2004) Identification and characterization of the FMO2 gene in *Rattus norvegicus*: a good model to study metabolic and toxicological consequences of the FMO2 polymorphism. *Pharmacogenetics* **14:**647–655.

Kim YM and Ziegler DM (2000) Size limits of thiocarbamides accepted as substrates by human flavin-containing monooxygenase 1. *Drug Metab Dispos* **28:**1003–1006.

Koukouritaki SB, Poch MT, Henderson MC, Siddens LK, Krueger SK, VanDyke JE, Williams DE, Pajewski NM, Wang T, and Hines RN (2007) Identification and functional analysis of common human flavin-containing monooxygenase 3 genetic variants. *J Pharmacol Exp Ther* **320:**266–273.

Krueger SK, Martin SR, Yueh MF, Pereira CB, and Williams DE (2002) Identification of active flavin-containing monooxygenase isoform 2 in human lung and characterization of expressed protein. *Drug Metab Dispos* **30:**34–41.

Krueger SK, Siddens LK, Henderson MC, Andreasen EA, Tanguay RL, Pereira CB, Cabacungan ET, Hines RN, Ardlie KG, and Williams DE (2005) Haplotype and functional analysis of four flavin-containing monooxygenase isoform 2 (FMO2) polymorphisms in Hispanics. *Pharmacogenet Genomics* **15:**245–256.

Krueger SK, Siddens LK, Martin SR, Yu Z, Pereira CB, Cabacungan ET, Hines RN, Ardlie KG, Raucy JL, and Williams DE (2004) Differences in *FMO2*1* allelic frequency between Hispanics of Puerto Rican and Mexican descent. *Drug Metab Dispos* **32:**1337–1340.

Krueger SK and Williams DE (2005) Mammalian flavin-containing monooxygenases: structure/function, genetic polymorphisms and role in drug metabolism. *Pharmacol Ther* **106:**357–387.

Larkin MA, Blackshields G, Brown NP, Chenna R, McGettigan PA, McWilliam H, Valentin F, Wallace IM, Wilm A, Lopez R, et al. (2007) Clustal W and Clustal X version 2.0. *Bioinformatics* **23:**2947–2948.

Malito E, Alfieri A, Fraaije MW, and Mattevi A (2004) Crystal structure of a Baeyer-Villiger monooxygenase. *Proc Natl Acad Sci U S A* **101:**13157–13162.

Nagata T, Williams DE, and Ziegler DM (1990) Substrate specificities of rabbit lung and porcine liver flavin-containing monooxygenases: differences due to substrate size. *Chem Res Toxicol* **3:**372–376.

Phillips IR and Shephard EA (2008) Flavin-containing monooxygenases: mutations, disease and drug response. *Trends Pharmacol Sci* **29:**294–301.

Poulsen LL and Ziegler DM (1979) The liver microsomal FAD-containing monooxygenase. Spectral characterization and kinetic studies. *J Biol Chem* **254:**6449–6455.

Rettie AE, Bogucki BD, Lim I, and Meier GP (1990) Stereoselective sulfoxidation of a series of alkyl p-tolyl sulfides by microsomal and purified flavin-containing monooxygenases. *Mol Pharmacol* **37:**643–651.

Sabourin PJ and Hodgson E (1984) Characterization of the purified microsomal FAD-containing monooxygenase from mouse and pig liver. *Chem Biol Interact* **51:**125–139.

Shehin-Johnson SE, Williams DE, Larsen-Su S, Stresser DM, and Hines RN (1995) Tissue-specific expression of flavin-containing monooxygenase (FMO) forms 1 and 2 in the rabbit. *J Pharmacol Exp Ther* **272:**1293–1299.

Siddens LK, Henderson MC, Vandyke JE, Williams DE, and Krueger SK (2008) Characterization of mouse flavin-containing monooxygenase transcript levels in lung and liver, and activity of expressed isoforms. *Biochem Pharmacol* **75:**570–579.

Suh JK, Poulsen LL, Ziegler DM, and Robertus JD (1999) Lysine 219 participates in NADPH specificity in a flavin-containing monooxygenase from *Saccharomyces cerevisiae*. *Arch Biochem Biophys* **372:**360–366.

van Berkel WJ, Kamerbeek NM, and Fraaije MW (2006) Flavoprotein monooxygenases, a diverse class of oxidative biocatalysts. *J Biotechnol* **124:**670–689.

van den Heuvel RH, Tahallah N, Kamerbeek NM, Fraaije MW, van Berkel WJ, Janssen DB, and Heck AJ (2005) Coenzyme binding during catalysis is beneficial for the stability of 4-hydroxyacetophenone monooxygenase. *J Biol Chem* **280:**32115–32121.

Veeramah KR, Thomas MG, Weale ME, Zeitlyn D, Tarekegn A, Bekele E, Mendell NR, Shephard EA, Bradman N, and Phillips IR (2008) The potentially deleterious functional variant flavin-containing monooxygenase *2*1* is at high frequency throughout sub-Saharan Africa. *Pharmacogenet Genomics* **18:**877–886.

Welch EM, Barton ER, Zhuo J, Tomizawa Y, Friesen WJ, Trifillis P, Paushkin S, Patel M, Trotta CR, Hwang S, et al. (2007) PTC124 targets genetic disorders caused by nonsense mutations. *Nature* **447:**87–91.

Whetstine JR, Yueh MF, McCarver DG, Williams DE, Park CS, Kang JH, Cha YN, Dolphin CT, Shephard EA, Phillips IR, et al. (2000) Ethnic differences in human flavin-containing monooxygenase 2 (FMO2) polymorphisms: detection of expressed protein in African-Americans. *Toxicol Appl Pharmacol* **168:**216–224.

Williams DE, Hale SE, Muerhoff AS, and Masters BS (1985) Rabbit lung flavin-containing monooxygenase. Purification, characterization, and induction during pregnancy. *Mol Pharmacol* **28:**381–390.

Yeung CK, Adman ET, and Rettie AE (2007) Functional characterization of genetic variants of human FMO3 associated with trimethylaminuria. *Arch Biochem Biophys* **464:**251–259.

Address correspondence to: Sharon K. Krueger, Linus Pauling Institute, Oregon State University, 571 Weniger Hall, Corvallis, OR 97331. E-mail: sharon.krueger@oregonstate.edu